

Microscopic structure of the DX center in Si-doped $Al_xGa_{1-x}As$: Observation of a vacancy by positron-annihilation spectroscopy

J. Mäkinen, T. Laine, K. Saarinen, and P. Hautojärvi

Laboratory of Physics, Helsinki University of Technology, 02150 Espoo, Finland

C. Corbel

Institut National des Sciences et Techniques Nucléaires, Centre d'Etudes Nucléaires de Saclay, 91191 Gif-sur-Yvette Cedex, France

V. M. Airaksinen

Laboratory of Electron Physics, Helsinki University of Technology, 02150 Espoo, Finland

J. Nagle

Laboratoire Central de Recherches, Thomson-CSF, 91404 Orsay Cedex, France

(Received 28 November 1994; revised manuscript received 24 April 1995)

Experimental results on the microscopic structure of the DX center in Si-doped $Al_xGa_{1-x}As$ are presented. Positron-annihilation spectroscopy indicates the vacancylike structure of the Si- DX center. The vacancy signal disappears persistently by illumination with infrared light. The optical cross section for this process is equal to the photoionization cross section for the Si- DX center. The critical temperature below which illumination makes the vacancy signal disappear is correlated to the persistent photoconductivity effect. We estimate the thermal ionization energy of the Si- DX center from positron experiments and demonstrate that thermal ionization of the DX center accounts for the disappearance of the vacancy at high temperatures. Temperature dependence of the positron trapping rate is typical of a negatively charged vacancy. The structural data from positron-annihilation spectroscopy are consistent with the vacancy-interstitial model that explains the metastability of the DX center in terms of two different lattice sites of the donor impurity.

I. INTRODUCTION

In GaAs and related compounds, substitutional group-IV impurities (Si, Ge, Sn) at the Ga site and group-VI impurities (S, Se, Te) at the As site form shallow donor states. However, irrespective of the nature of the donor species, they also give rise to deep electron levels known as DX .^{1,2} In GaAs the DX level is a resonant state in the conduction band, but in $Al_xGa_{1-x}As$ it becomes the lowest-energy state of the donor when the AlAs mole fraction is $x > 0.22$. In this range of the alloy composition the capture of electrons into the deep level reduces the number of electrons in the conduction band, and controls the conductivity of n -type material. At low temperatures optical ionization of the DX center leads to persistent photoconductivity, with electrons remaining in the conduction band. Because of these two circumstances, defect metastability associated with an isolated substitutional impurity atom and the deleterious consequences for semiconductor devices, a considerable amount of effort has been directed at understanding the fundamental properties of donors in III-V semiconductor alloys.^{3,4}

The picture of electron capture at the DX level was developed by Lang and co-workers.^{1,2} They found that electron capture at the DX level is thermally activated, and that the capture cross section is exceedingly small ($< 10^{-30}$ cm²) below 70 K. Electron capture was ex-

plained in terms of multiphonon emission. They also found that the energy for optical ionization of the DX level (optical depth ~ 1.0 eV) is much larger than its thermal ionization energy (thermal depth ~ 0.1 eV). This large Stokes shift cannot be reconciled with the effective-mass theory for impurities in semiconductors. These findings, supported and refined by later experiments, were advanced as an indication of two different structural configurations of the donor.¹⁻³

A strong boost to understanding the metastability of the DX center comes from theoretical studies.⁵⁻¹⁰ They have given an indication that an isolated donor impurity may undergo a shallow-to-deep transition. From total-energy calculations, a metastable state is found for the negatively charged donor.⁷ The calculated atomic structure is characterized by a large (> 1 Å) displacement of the column-IV donor atom in the $\langle 111 \rangle$ direction into a threefold-coordinated position. In the case of Si, the geometry can be viewed as a pair of a Ga vacancy and a Si interstitial. In the distorted configuration the bonding is large sp^2 -like. Theoretical studies therefore suggest that different forms of sp hybridization in covalent crystals are responsible for the metastability of the donor impurities. This explanation implies that this type of defect metastability in semiconductors may be more common than expected so far. The same basic mechanism has been used to explain the metastability of the EL2 center in GaAs.^{5,6} Recently the DX -like center was also predict-

ed in some II-VI compounds.¹¹ It has become increasingly evident that the vacancy-inertial model is consistent with the electrical and optical properties of the *DX* center.⁹ Nevertheless, there is very little direct structural data about the *DX* center.

We address the microscopic structure of the *DX* center in $\text{Al}_x\text{Ga}_{1-x}\text{As}$ using positron-annihilation spectroscopy. The discovery that a positron can become localized at vacancies has led to a highly versatile method for the study of atomic-scale defects in solids.^{12,13} The potential benefit of this technique is that vacancies can be unambiguously distinguished from other types of defects. The annihilation rate of a positron quantifies directly the electron density. The Doppler broadening of the annihilation radiation gives information about the momentum distribution of annihilating electrons. Both techniques can be used to detect vacancies in semiconductors if the vacancy concentration is larger than 10^{15} cm^{-3} .

Positron-annihilation measurements have indicated the vacancylike structure of the *DX* center in $\text{Al}_x\text{Ga}_{1-x}\text{As}$.¹⁴ It has provided a direct indication of the change in the structural configuration of the donor associated with electron transfer from the shallow donor state to the deep *DX* state. Positron-annihilation experiments have also pointed out the close similarity between the *DX* center and the metastable state of the EL2 center in GaAs.^{15,16}

This work completes preliminary results published earlier.¹⁴ Here we discuss thoroughly the results of positron-annihilation experiments and their interpretation. Experimental results are presented in Sec. III. The properties of the vacancy in Si-doped $\text{Al}_x\text{Ga}_{1-x}\text{As}$ are compared in detail with some of the well-established properties of the Si-*DX* center (Sec. V). That comprises the optical and thermal ionization of the *DX* center, and the influence of the alloy composition on the thermal activation energy for electron capture at the *DX* center. Additional results on the temperature dependence of the positron trapping rate indicating the negative-charge state of the vacancy are presented. Information about the local structure and the charge state of the Si-*DX*

center is discussed in Sec. VI. The structural data from positron-annihilation spectroscopy is consistent with the vacancy-interstitial model which explains the metastability of the *DX* center in terms of two different lattice sites of the donor impurity.

II. EXPERIMENTAL DETAILS

Positron annihilation was studied in undoped and *n*-type $\text{Al}_x\text{Ga}_{1-x}\text{As}$ layers. The *n*-types layers were doped with Si, which is a column-IV donor at the Ga site. In addition, Si-doped *n*-type and Be-doped *p*-type GaAs layers were measured as references. All layers were grown using a conventional molecular-beam-epitaxy (MBE) system.

In the Si-doped $\text{Al}_x\text{Ga}_{1-x}\text{As}$ layers the AlAs mole fraction varies from $x=0.18$ to 0.61 (Table I). The substrate was *n* type ($x=0.18$ and 0.33) or undoped semi-insulating ($x=0.23$, 0.29 , and 0.61) GaAs(100). The buffer layer was either *n*-type GaAs ($x=0.18$ and 0.33), undoped GaAs followed by $\text{Al}_x\text{Ga}_{1-x}\text{As}$ ($x=0.23$ and 0.61), or GaAs followed by a GaAs/AlAs superlattice ($x=0.29$). The thickness of the *n*-type $\text{Al}_x\text{Ga}_{1-x}\text{As}$ layers is $2 \mu\text{m}$ ($x=0.18-0.33$) or approximately $1 \mu\text{m}$ ($x=0.61$), and all structures are covered by a 50–100-Å-thick *n*-type GaAs cap layer. For the layers $x=0.23$, 0.29 , and 0.61 , the Al fraction was determined by double x-ray diffraction. The Si concentration is $N_D \approx 2.5 \times 10^{18} \text{ cm}^{-3}$ in the layers $x=0.18-0.33$. In the layer $x=0.61$ the Si concentration is approximately 10^{18} cm^{-3} .

In the undoped $\text{Al}_x\text{Ga}_{1-x}\text{As}$ layers the AlAs mole fractions are $x=0.11$, 0.25 , and 0.32 , and the layer thickness varies from 1.5 to $2.7 \mu\text{m}$. Unintentional doping makes the layers weakly *p*-type. In the GaAs layers the Si and Be concentrations are $[\text{Si}] = 4 \times 10^{18} \text{ cm}^{-3}$ and $[\text{Be}] = 4 \times 10^{16} \text{ cm}^{-3}$.

Positron annihilation in the epitaxial layers was investigated using the low-energy positron beam technique.¹⁷ The 511-keV annihilation line was measured at an incident positron energy which was chosen between 15 and

TABLE I. The AlAs mole fractions x , Si concentrations (Si), the Hall carrier concentrations n_H at 300 K, and the layer thicknesses in the GaAs and $\text{Al}_x\text{Ga}_{1-x}\text{As}$ samples. All layers were grown by conventional molecular-beam epitaxy on GaAs(100) substrates. The AlAs fraction in the layers $x=0.23$, 0.29 , and 0.61 was determined by x-ray diffraction. The layers were grown either in (a) Helsinki University of Technology, (b) Thomson-CSF, (c) Université des Sciences et Techniques de Lille, or (d) Tampere University of Technology.

x	Dopant	[Si] cm^{-3}	n_H cm^{-3}	Layer thickness μm	Place of growth
<i>n</i> -GaAs	Si	4×10^{18}		2	<i>d</i>
<i>p</i> -GaAs	Be		4×10^{16}	2	<i>a</i>
0.11	undoped			1.6	<i>c</i>
0.25	undoped			2.7	<i>c</i>
0.32	undoped			2	<i>d</i>
0.18	Si	2.5×10^{18}		2	<i>a</i>
0.23	Si	2.5×10^{18}	2.3×10^{18}	2	<i>a</i>
0.29	Si	2.5×10^{18}	6.1×10^{17}	2	<i>a</i>
0.33	Si	2.5×10^{18}	3×10^{17}	2	<i>a</i>
0.61	Si	$\sim 1 \times 10^{18}$	2×10^{17}	1	<i>b</i>

23 keV. These energies correspond to the mean positron stopping depths of 0.5 and 1.0 μm in GaAs. In each case it was verified that contributions from the annihilation events at the surface and in the substrate were negligible. Typically 5×10^6 counts were collected to the annihilation peak. The sample temperature was controlled between 20 and 300 K with a closed-cycle He cryocooler and a resistive heater, and measured with a silicon diode temperature sensor. Above room temperature the sample was heated with an electron-beam heater, and temperature was measured with a type-*K* thermocouple mounted to the sample surface. A GaAs infrared (IR) light-emitting diode was used for illumination (photon energy ~ 1.3 eV). The light intensity measured with a Ge photodetector was typically 0.1 mW/cm^2 .

Observation of positron trapping at vacancy defects is based on the Doppler broadening of the annihilation radiation.¹² Momentum of the annihilating electron causes a shift in the energy of the photon, $\Delta E = \frac{1}{2}cp_L$, where p_L is the momentum component of the electron-positron pair parallel to the direction of photon emission, and c is the speed of light. The shape of the 511-keV annihilation line, convoluted with the resolution of the Ge detector, can be described in terms of valence and core electron annihilation. One can distinguish between the low-momentum part of the spectrum, which arises mainly from the valence electron annihilation, and the high-momentum part arising from the core electrons. The low-momentum part is characterized by the valence-annihilation parameter S , which is defined as the number of annihilation events over the energy range $511 \text{ keV} \pm \Delta E$ ($\Delta E = 0.95 \text{ keV}$) around the centroid of the peak. It represents the fraction of electron-positron pairs with a longitudinal momentum component $p_L \leq 0.5$ a.u. ($p_L/m_0c \leq 3.7 \times 10^{-3}$, where m_0 is the electron mass). The core-annihilation parameter W is calculated from the tail of the peak, $2.9 \text{ keV} \leq |\Delta E| \leq 7.3 \text{ keV}$. As defined here, it corresponds to annihilations with a large momentum component p_L between 1.6 and 3.9 a.u. (or $1.1 \times 10^{-2} \leq p_L/m_0c \leq 2.8 \times 10^{-2}$) which are entirely due to the core electrons. It appeared that in case of the vacancy defects in *n*-type $\text{Al}_x\text{Ga}_{1-x}\text{As}$ the change in valence electron annihilation is rather small. Therefore the core-annihilation parameter W will be used in the most part of this work.

III. VACANCIES IN $\text{Al}_x\text{Ga}_{1-x}\text{As}$: EXPERIMENTAL RESULTS

A. Observation of vacancies in Si-doped $\text{Al}_x\text{Ga}_{1-x}\text{As}$

p-type GaAs and undoped $\text{Al}_x\text{Ga}_{1-x}\text{As}$ layers are used as a reference for free positron annihilation.¹⁴ In *p*-type GaAs, only free positron annihilation is seen from 20 K to room temperature. It was directly verified by making comparison with liquid-encapsulated-Czochralski (LEC)-grown *p*-type GaAs. The annihilation parameters in the MBE-grown Be-doped layer are identical with those in Zn-doped ($5 \times 10^{17} \text{ cm}^{-3}$) LEC-GaAs, in which the positron lifetime 231 ± 1 ps is equal to the free positron lifetime in GaAs.¹⁸ It is also a general observation that va-

cancies are not seen by positron spectroscopy in as-grown *p*-type GaAs.^{18,19}

In $\text{Al}_x\text{Ga}_{1-x}\text{As}$ the core-annihilation parameter varies with the alloy composition (Fig. 1). It can be traced back to a smaller number of positrons annihilating with the core electrons when Ga, the 3*d* core shell of which makes a major contribution to the core annihilation, is replaced by Al. This can be demonstrated by comparing the theoretical annihilation rates in GaAs and AlAs.²⁰ The total annihilation rates $\lambda_t = 4.44 \text{ ns}^{-1}$ in GaAs and 4.29 ns^{-1} in AlAs are nearly identical. However, the annihilation rate with the core electrons in GaAs, $\lambda_c = 0.12\lambda_t$, is larger by a factor of 2 than in AlAs ($\lambda_c = 0.06\lambda_t$). In these annihilation rates the core contribution includes the As and Ga 3*d* electrons and all the inner electron shells.

The increase of temperature from 20 K to room temperature causes a small and nearly linear decrease of the core annihilation parameter in *p*-type GaAs and in undoped $\text{Al}_x\text{Ga}_{1-x}\text{As}$.¹⁴ This is typical of free positron annihilation, and can be related to thermal lattice expansion.²¹

In the *n*-type layers the concentration of Si atoms is $N_D \approx 2.5 \times 10^{18} \text{ cm}^{-3}$, apart from the layer with the highest AlAs fraction $x = 0.61$ (Table I). In the Si-doped layer $x = 0.29$ the Hall carrier concentration at room temperature $n_H = 6 \times 10^{17} \text{ cm}^{-3}$ is clearly lower than in *n*-type GaAs:Si ($n_H = 2.4 \times 10^{18} \text{ cm}^{-3}$) grown under similar conditions. In the Si-doped layer $x = 0.61$ the Hall carrier concentration at room temperature is $n_H = 2 \times 10^{17} \text{ cm}^{-3}$, and it decreases by one order of magnitude by 77 K. These properties are indicative of the electron capture at the *DX* level, and they are observed quite generally at the alloy compositions at which the *DX* level is the lowest state of the donor impurity.³

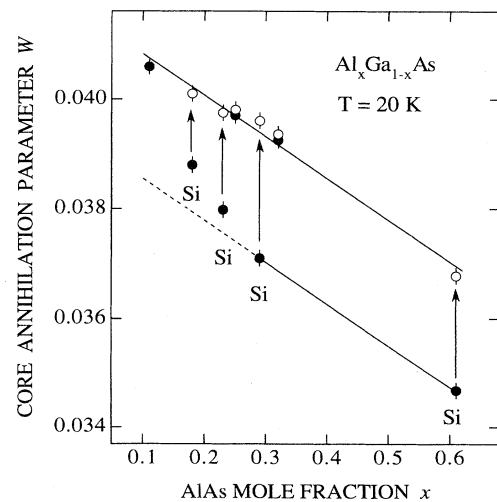


FIG. 1. The core-annihilation parameter W in undoped and Si-doped $\text{Al}_x\text{Ga}_{1-x}\text{As}$ layers at different alloy compositions. The core-annihilation parameters were measured in the dark at 20 K before (●) and after (○) illumination with 1.3-eV photons from a GaAs infrared light-emitting diode.

The core-annihilation parameters in the Si-doped layers $x = 0.18, 0.23, 0.29,$ and 0.61 measured at 20 K after cooling the samples in the dark are plotted in Fig. 1. When compared to undoped $\text{Al}_x\text{Ga}_{1-x}\text{As}$ at the same alloy composition, the core-annihilation parameters in the Si-doped layers are systematically smaller. The temperature dependence of positron annihilation gives a further indication of the different positron states in undoped and Si-doped $\text{Al}_x\text{Ga}_{1-x}\text{As}$. In the layer $x = 0.29$ the core-annihilation parameter was found to be independent of temperature between 20 and 300 K.¹⁴ As in the layer $x = 0.29$, the core-annihilation parameter is constant below 300 K in the layer in which the AlAs fraction is $x = 0.61$. The temperature dependence in the layers with a small AlAs fraction ($x < 0.25$) is studied in detail in Sec. III C, and at this point we just note that the core-annihilation parameter is also lower than in undoped $\text{Al}_x\text{Ga}_{1-x}\text{As}$ in all Si-doped layers at room temperature. The defect state disappears reversibly at high temperatures. The strong increase of the core-annihilation parameter in the layer $x = 0.29$ between 350 and 550 K makes the core-annihilation parameters in Si-doped and undoped layers identical in the high-temperature limit.¹⁴ A similar increase of the core-annihilation parameter is observed in the Si-doped layer $x = 0.23$ from 300 to 550 K, and will be discussed in more detail in Sec. V C.

The Doppler parameters in Si-doped $\text{Al}_x\text{Ga}_{1-x}\text{As}$ signify a positron state which is characterized by reduced probability of core electron annihilation. It gives an indication of positron annihilation at vacancy-type defects. The reduced number of core-electron-annihilation events is due to a smaller overlap of the positron wave function with the ion cores when the positron is trapped at a vacancy. Positron annihilation therefore demonstrates that Si-doped $\text{Al}_x\text{Ga}_{1-x}\text{As}$ with $x \geq 0.18$ contains vacancies. The change of the core-annihilation parameter compared to free positron annihilation at the same alloy composition is smaller in the layers $x = 0.18$ or 0.23 than at higher Al concentrations (Fig. 1). However, in all $\text{Al}_x\text{Ga}_{1-x}\text{As}$ layers the vacancy signal disappears after exposure to IR light (Sec. III B), indicating that the same defect is observed in all Si-doped layers.

In summary, we conclude that Si-doped layers contain a vacancy defect which cannot be detected in undoped $\text{Al}_x\text{Ga}_{1-x}\text{As}$. The vacancy signal disappears in thermal equilibrium above 300 K. These vacancy defects can be distinguished from vacancies in GaAs (Refs. 18 and 22) by their properties which appear when the layers are illuminated.

B. Removal of the vacancy signal by illumination

Optical ionization of the Si-DX center at low temperatures ($T < 80$ K) gives rise to persistent photoconductivity with electrons remaining in the conduction band or, when the $\text{Al}_x\text{Ga}_{1-x}\text{As}$ alloy has an indirect band gap, to capture of electrons at shallow donor states. Illumination of the $\text{Al}_x\text{Ga}_{1-x}\text{As}$ layers with IR light from GaAs light-emitting diodes at 20 K makes the vacancy signal

disappear.¹⁴ A most interesting observation is that this phenomenon is persistent. The photoeffect lasts at least several days unless the temperature is increased, and it is observed in all Si-doped $\text{Al}_x\text{Ga}_{1-x}\text{As}$ layers ($x \geq 0.18$).

The core-annihilation parameter in the Si-doped layer $x = 0.29$ is plotted as a function of the illumination time for two different light intensities in Fig. 2. The measurement was done in the dark after each illumination. The core-annihilation parameter shows a persistent light-induced increase. After a sufficiently long period of light exposure, it reaches a well-defined constant value whereafter further illumination does not influence positron annihilation. The saturation levels, which depend on the Al concentration of the layer, are indicated in Fig. 1. In all n -type Si-doped layers the core-annihilation parameter after the light exposure becomes identical with those measured in undoped $\text{Al}_x\text{Ga}_{1-x}\text{As}$. This leads to a simple interpretation of the photoeffect. Exposure to IR light evidently transfers the vacancies into a state in which they no longer act as a positron trap.

To compare layers with different alloy compositions, we make use of the ratio W/W_B which yields the change in the core-annihilation parameter due to positron trapping. The core-annihilation parameter after illumination yields directly the value W_B for free positron annihilation in the n -type $\text{Al}_x\text{Ga}_{1-x}\text{As}$ layers. The core-annihilation parameter in the Si-doped layers at 20 K are $W(20\text{ K})/W_B(20\text{ K}) = 0.975(3)$ for $x = 0.18$, $0.955(3)$ for $x = 0.23$, $0.936(3)$ for $x = 0.29$, and $0.937(3)$ for $x = 0.61$. The light-induced change in positron annihilation can be seen also in the valence-annihilation parameter S from the same series of measurements. The increase of the valence-annihilation parameter due to positron trapping is $S(20\text{ K})/S_B(20\text{ K}) = 1.0039(5)$ in the layer $x = 0.29$, and $1.0041(5)$ for the higher AlAs fraction $x = 0.61$. In

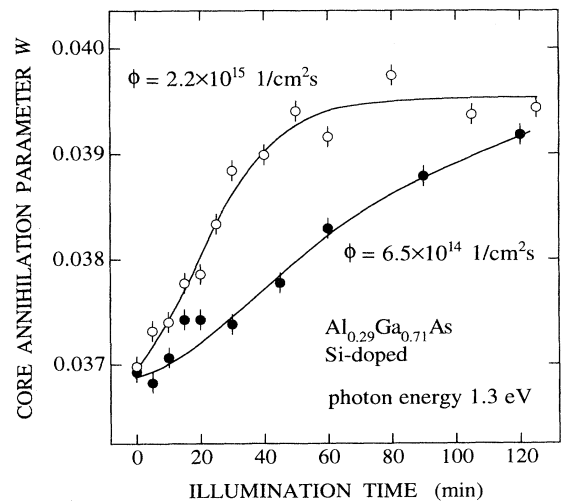


FIG. 2. Plot of the core-annihilation parameter W vs time of illumination in a Si-doped $\text{Al}_x\text{Ga}_{1-x}\text{As}$ layer $x = 0.29$ at two different light intensities 6×10^{14} and 2.2×10^{15} photons/cm²s (photon energy ~ 1.3 eV).

the layers $x = 0.29$ and 0.61 the ratios W/W_B are identical, although the core-annihilation parameters vary with the AlAs fraction. At low Al concentrations ($x < 0.25$) positron trapping at vacancies causes a smaller change in the core-annihilation parameter W/W_B . It will be attributed to a smaller vacancy concentration in the layers $x = 0.18$ and 0.23 .

The light-induced increase of the core-annihilation parameter in the Si-doped layer $x = 0.33$ at 20 K is small compared to the layers $x = 0.29$ and 0.61 . This is due to the increase of the core-annihilation parameter in the dark from 200 to 100 K in this particular sample. It is typical of negatively charged ions which can support localized Rydberg states for positrons.^{18,22} Such defects act as competitive trapping centers at low temperatures. When the core-annihilation parameter W is taken at 300 K in the layer $x = 0.33$, we find $W(300 \text{ K})/W_B = 0.935(5)$ which is the same as in the layers $x = 0.29$ and 0.61 .

In the undoped layers the core-annihilation parameters before and after illumination are identical (Fig. 1). Measurement during light exposure also yields the same Doppler parameters.

Disappearance of the vacancy signal after illumination, which was demonstrated at 20 K in Fig. 1, is persistent to considerably higher temperatures. Figure 3 shows the

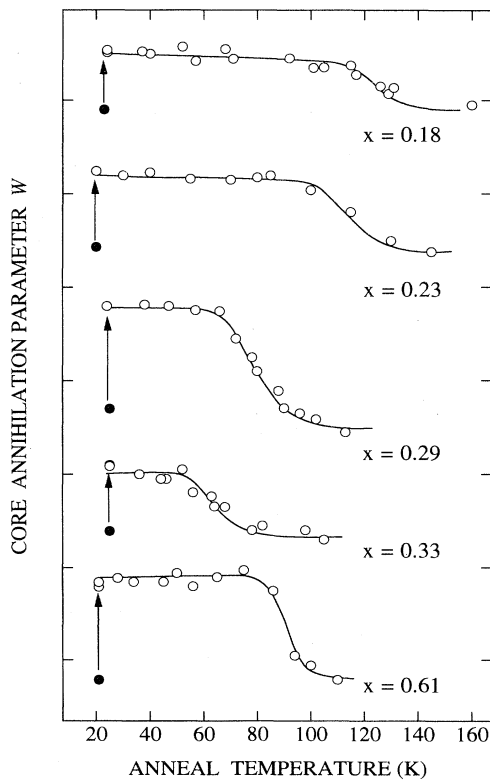


FIG. 3. Plot of the core-annihilation parameter W vs anneal temperature showing the influence of the alloy composition on the recovery of the vacancy signal in Si-doped $\text{Al}_x\text{Ga}_{1-x}\text{As}$ after illumination at 20 K. The arrows indicate the increase of the core-annihilation parameter due to illumination.

light-induced increase of the core annihilation parameter in the Si-doped layers at 20 K, and its evolution as temperature is subsequently raised. In the layer $x = 0.29$, the core-annihilation parameter after exposure to IR light is indicative of free positron annihilation up to 70 K. Thereafter the vacancy signal recovers, and by 90 K the core-annihilation parameter returns to the level before illumination. Another observation is that the critical temperature below which the vacancy signal can be persistently removed depends on the alloy composition (Fig. 3). For $x = 0.18$, the vacancy signal after illumination recovers between 120 and 140 K, whereas it occurs already above 50 K for $x = 0.33$. Clearly, at this range of the alloy composition, increase of the AlAs mole fraction lowers the critical temperature. At a still higher Al concentration corresponding to $x = 0.61$ the critical temperature increases again compared to the $x = 0.33$ layer. Measurements at the annealing temperature and at $T = 20 \text{ K}$ yield very similar stages of recovery of the vacancy signal.

Positron annihilation was also measured in an n -type MBE-grown Si-doped ($[\text{Si}] = 4 \times 10^{18} \text{ cm}^{-3}$) GaAs layer. Unlike the p -type MBE-grown layer or Zn-doped LEC-grown GaAs, the n -type layer contains vacancies which are detected by positron annihilation. However, contrary to Si-doped $\text{Al}_x\text{Ga}_{1-x}\text{As}$ ($x \geq 0.18$), this vacancy does not show any photoeffects at 20 K, indicating that it is different from the defects in the $\text{Al}_x\text{Ga}_{1-x}\text{As}$ layers. Typical values for the core-annihilation parameters at vacancies in GaAs (Refs. 15 and 23) and the trapping coefficient for positron capture at vacancies in semiconductors ($1 \times 10^{15} \text{ s}^{-1}$ at 300 K) yield an estimate of $\sim 10^{16} \text{ cm}^{-3}$ for the vacancy concentration in the Si-doped GaAs layer.

C. Temperature dependence of the Doppler line-shape parameters at $T < 150 \text{ K}$

The temperature dependence of positron annihilation was measured in greater detail in the Si-doped $\text{Al}_x\text{Ga}_{1-x}\text{As}$ layers $x = 0.18, 0.23$, and 0.29 below 150 K. The aim is to find the temperature dependence of the positron trapping rate at the vacancy to obtain information about the charge state of the vacancy.

We first consider the temperature range from 20 to 100 K. The temperature dependence of the core-annihilation parameter in different layers is plotted in Fig. 4. Positron annihilation was measured at each temperature after cooling the sample in the dark. The temperature dependence of free positron annihilation $W_B(T)$ in this temperature range was measured after illuminating the samples at 20 K. To compare layers with different alloy compositions we make use of the ratios $W(T)/W_B(20 \text{ K})$.

In the layer $x = 0.29$ the core-annihilation parameter is totally independent of temperature. This is the case also in the Si-doped layer with a higher AlAs fraction $x = 0.61$ from 20 to 300 K (not shown). In the layers in which the AlAs mole fraction is lower ($x < 0.25$), the core-annihilation parameters are clearly temperature dependent. The decrease of the core-annihilation param-

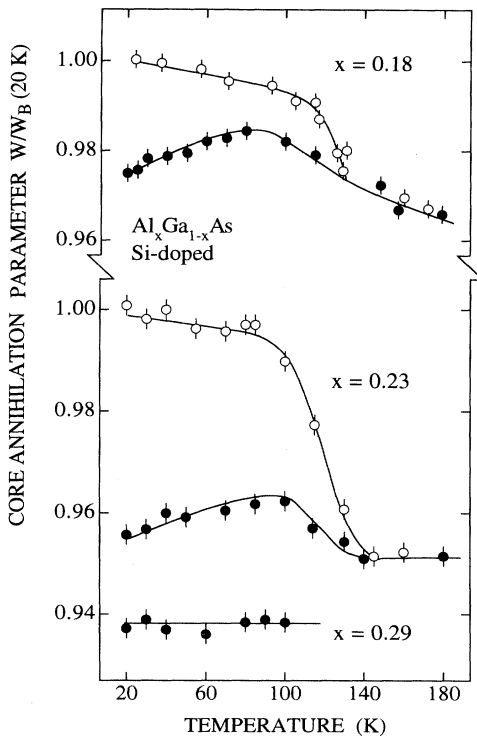


FIG. 4. Plot of the core-annihilation parameter vs temperature at $T \leq 150$ K in Si-doped $\text{Al}_x\text{Ga}_{1-x}\text{As}$ layers $x = 0.18$, 0.23, and 0.29 measured after cooling the samples in the dark (\bullet) and after illumination with infrared light at 20 K (\circ). The figure shows the ratios W/W_B where W_B is the core-annihilation parameter measured in each layers at 20 K after illumination.

eter from 100 to 20 K indicates that an *increasing* fraction of positrons annihilates at the vacancies. We will argue (Sec. VI B) that this is due to the negative charge of the vacancy.

From 100 to 150 K the core-annihilation parameter decreases in the layers $x = 0.18$ and 0.23, and thereafter it remains almost constant up to room temperature. Such temperature dependence suggests that in addition to the vacancy defects there are some other positron traps. The possible origin of the temperature dependence and its influence on the interpretation of the experimental results at $T < 100$ K is discussed in Sec. VI B.

IV. KINETIC POSITRON TRAPPING MODEL

Positrons entering a solid are reduced to thermal energies in a time which is much shorter than the lifetime against annihilation. Following thermalization, positrons in a defect-free crystal are delocalized and annihilate at a rate $\lambda_B = \tau_B^{-1}$, where τ_B is the free positron lifetime. In a defected crystal localized states may form as a result of positron trapping at vacancy defects. The positron population is then distributed between various states. The experimental core-annihilation parameter is

$$W = \left[1 - \sum_i \eta_i \right] W_B + \sum_i \eta_i W_{Di}, \quad (1)$$

where η_i is the fraction of positrons annihilating from the defect state i , the subscript B refers to free positron annihilation, and D to the defect state. Around a vacancy defect the electron density and particularly the core electron density is reduced. Thus, inevitably, the core-annihilation parameter which gives a measure of the core electron annihilation decreases when there is appreciable positron trapping in a crystal.

The kinetic trapping model²⁴ assumes that initially all positrons exist in a single delocalized state from which they either annihilate at the rate λ_B or make a transition with a time-independent rate κ_i to a defect state. The fraction of positrons annihilating from each state is given by

$$\eta_i = \frac{\kappa_i}{\lambda_B + \sum_j \kappa_j}. \quad (2)$$

In a more general model, it is also possible to include thermal detrapping from states in which the positron binding energy is small. The positron trapping rate from the free positron state to a defect state is proportional to the concentration of defects,

$$\kappa = \mu C_D. \quad (3)$$

Equation (3) defines the positron trapping coefficient μ (trapping rate per unit atomic concentration of defects).

Positron trapping becomes observable whenever the trapping rate is comparable to the free positron-annihilation rate, and W_D is sufficiently different from W_B . In semiconductors the positron trapping coefficient at neutral and negatively charged vacancies varies typically from 10^{15} to $5 \times 10^{16} \text{ s}^{-1}$,^{25,28} depending on the charge of the vacancy and temperature. This means that vacancies can be detected when their concentration is higher than 10^{15} cm^{-3} .

V. CORRELATION OF THE VACANCY WITH THE DX CENTER

We are now in a position to correlate the properties of the vacancy with the DX center. It is the persistent photoinduced removal of the vacancy signal that suggests positron trapping at the DX center.¹⁴ In this section we will present a detailed analysis of the experimental results, and compare the properties of the vacancy with some of the well-established electrical and optical properties of the Si- DX center. For that purpose we will examine the optical ionization process, and consider the effect of the alloy composition on the activation energy for electron capture at the DX level. At high temperatures the disappearance of the vacancy will be shown to coincide with the thermal ionization of the DX center.

A. Removal of the vacancy and optical ionization of the DX center

In this section we compare the disappearance of the vacancy signal due to illumination, and the optical ionization of the DX center. The optical cross section for the removal of the vacancy signal is estimated from the positron trapping rate κ . As long as the trapping coefficient μ is constant, κ directly yields the time variation of the number of defects C_D . The fact that after illumination only free positron annihilation is seen in the Si-doped layers implies that there are no other vacancy defects to trap positrons. Therefore we consider only these two states, and calculate the trapping rate at the vacancy from the trapping model as

$$\kappa = \lambda_B \frac{W - W_B}{W_D - W} \quad (4)$$

For Si-doped $\text{Al}_x\text{Ga}_{1-x}\text{As}$ with $x=0.29$ the core-annihilation parameters as a function of the illumination time were given in Fig. 2. Figure 5 shows the trapping rate calculated from that data. We assume that the core-annihilation parameter before illumination is equal to W_D , i.e., that all positrons annihilate at the vacancy defects (see Sec. VI A).

The decay of the trapping rate and therefore also the vacancy concentration can be fit by a single exponential function

$$\frac{\kappa}{\kappa_0} = \frac{C_D}{C_{D0}} = \exp(-\sigma\phi t) \quad (5)$$

as κ decreases from approximately $10\lambda_B$ to $0.1\lambda_B$. Here

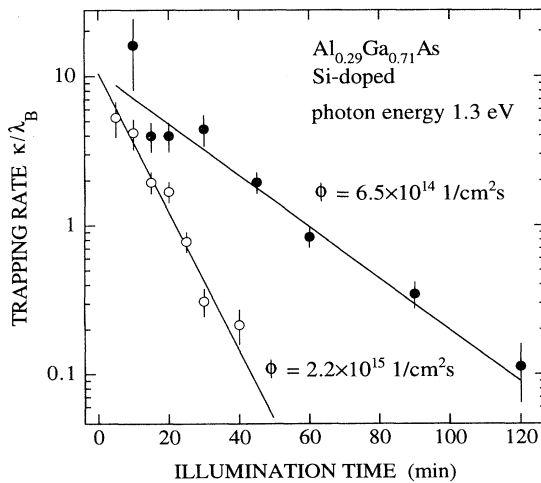


FIG. 5. The positron trapping rate κ in units of the free positron-annihilation rate λ_B as a function of illumination time in the Si-doped $\text{Al}_x\text{Ga}_{1-x}\text{As}$ layer $x=0.29$ at two different light intensities 6.5×10^{14} and 2.2×10^{15} photons/cm²s. The solid lines indicate the exponential decay of the trapping rate with the time constant $(\sigma\phi)^{-1} = 1.5 \times 10^3$ and 5.6×10^2 s.

ϕ is the light intensity in photons/cm²s. The cross section, which is obtained from the time constants $(\sigma\phi)^{-1}$ of the transients when ϕ is known, is $\sigma = (0.9 \pm 0.2) \times 10^{-18}$ cm² at 20 K. The two light intensities yield identical values for the cross section.

The optical ionization cross section for the DX center in Si-doped $\text{Al}_x\text{Ga}_{1-x}\text{As}$ has been measured at different photon energies using photocapacitance techniques.^{29,30} From that data the optical ionization cross section $\sigma_0 = 1 \times 10^{-18}$ cm² at the photon energy 1.3 eV at 80 K for the DX center in Si-doped $\text{Al}_x\text{Ga}_{1-x}\text{As}$ with $x=0.30$ can be estimated. The variation of the optical ionization cross section with temperature is weak at low temperatures,³¹ justifying a direct comparison with the positron experiments at 20 K. Within the experimental error, the cross section estimated from the positron trapping rate is equal to the optical ionization cross section of the Si- DX center. It shows that when the DX centers are ionized, the same proportion of vacancies disappears. We also note that the cross sections are both much smaller than what is typically found for deep levels in semiconductors.³²

Optical ionization of the vacancy, if it makes the vacancy positively charged or changes the ionic structure of the center, would explain the disappearance of the vacancy signal after light exposure. Since it is the only known defect in $\text{Al}_x\text{Ga}_{1-x}\text{As}$ which is persistently ionized by illumination, the defect state was associated with positron annihilation at the DX center.¹⁴ The detailed comparison of the optical ionization cross sections strongly supports this identification. It is also consistent with the charge state of the DX center.^{3,4} One or two electrons occupy the DX level in the ground state, and it is either neutral or negatively charged. In either case the charge of the DX center makes it a potential trapping center.

B. Recovery of the vacancy signal and persistent photoconductivity

The critical temperature below which the persistent photoconductivity in n -type $\text{Al}_x\text{Ga}_{1-x}\text{As}$ is observed varies significantly with the donor species and the alloy composition.^{3,4} The reappearance of the vacancy after photoexcitation occurs at the same temperature as the decay of the persistent photoconductivity.¹⁴ The correlation between the vacancy and the DX center is even more detailed, as one can see by looking at the effect of the alloy composition.

It has been found earlier that the activation energy for electron capture at the DX level varies significantly with the AIAs mole fraction. In Si-doped $\text{Al}_x\text{Ga}_{1-x}\text{As}$ a distribution of DX levels has been resolved.³³⁻³⁵ In Fig. 6 we show the average capture barrier measured in modulation-doped field-effect transistors and diodes using deep-level transient spectroscopy (DLTS) by Mooney, Caswell, and Wright.³³ The average barrier for electron capture has a minimum value of 0.21 eV at $x \approx 0.35$ which is near the crossover from direct to indirect band gap. At lower Al concentrations the barrier increases steeply, and it is approximately 0.4 eV at $x = 0.27$.³³ For larger AIAs mole fractions $x > 0.35$, the capture barrier

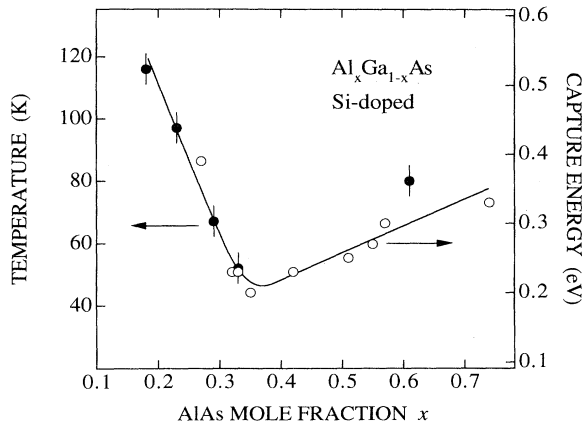


FIG. 6. Plot showing the influence of alloy composition on the anneal temperature at which the vacancy signal first appears after photoquenching at 20 K. The temperatures were estimated from the core-annihilation parameter vs anneal temperature plots shown in Fig. 3. The activation energies for electron capture at the Si- DX center are from Ref. 33.

increases again.

Here we find a systematic decrease of the temperature at which the vacancy signal appears when the AlAs fraction increases from $x = 0.18$ to $x = 0.33$. Figure 6 shows the temperature for the onset of the recovery of the vacancy signal after exposure to IR light at 20 K estimated from the experimental data in Fig. 3. The influence of the carrier concentration on the electron-capture rate is unimportant as the Si concentrations in the layers are very similar. For $x = 0.23$ the vacancy signal can be first seen at $T = 100$ K, whereas for $x = 0.33$, which is close to the Al concentration yielding the minimum for the capture barrier, the recovery starts already at $T = 50$ K. This is consistent with the variation of the electron-capture barrier with the alloy composition. For $x = 0.61$ the recovery starts at $T = 80$ K. This also corresponds very well to the increase of the electron-capture barrier when the AlAs fraction is $x > 0.35$. Evidently, electron capture at the Si- DX center^{33,36} can be used to explain the temperature at which the vacancy signal appears in different $Al_xGa_{1-x}As$ layers.

C. Positron trapping at vacancies and thermal ionization of the DX center

In the previous sections, the persistent disappearance of the vacancy signal was related to optical ionization of the DX center. Below we will demonstrate that the thermal ionization of the DX center can explain the temperature dependence of the core-annihilation parameter at $T > 300$ K.

We first consider the Si-doped layer with $x = 0.29$. The Hall carrier concentration $n_H = 6 \times 10^{17} \text{ cm}^{-3}$ at room temperature is much smaller than the concentration of donor atoms, $[Si] \approx 2.5 \times 10^{18} \text{ cm}^{-3}$. Most of the DX centers are therefore occupied by electrons at 300 K.

In positron experiments the vacancy signal disappears between 300 and 600 K. This is the same temperature range at which the DX centers are ionized by thermal emission of electrons from the deep donor level.¹⁴

To make this argument more quantitative, we calculate the core-annihilation parameter assuming that the DX center acts as a positron trap when the deep level is occupied, and compare it with the experiment. The occupation of the DX level is derived from the two-level model which was applied by Theis, Mooney, and Parker³⁷ in explaining their Hall data in Si-doped $Al_xGa_{1-x}As$. Below we briefly outline the calculation in case of two-electron occupation of the DX level.

We consider a donor atom which gives rise to a shallow hydrogenic level and a deep level. If the total number of donor atoms is N_D , the concentrations of ionized shallow donors (n_d^+) and the donors with electrons at the deep level (n_{DX}^-) are given by

$$n_d^+ = \frac{N_D}{1 + \exp[(E_h - E_F)/kT] + \exp[2(E_{DX} - E_F)/kT]}, \quad (6a)$$

$$n_{DX}^- = \frac{N_D \exp[2(E_{DX} - E_F)/kT]}{1 + \exp[(E_h - E_F)/kT] + \exp[2(E_{DX} - E_F)/kT]}. \quad (6b)$$

The energy for the transfer of an electron from the DX level to the edge of the conduction band may be written in terms of the ionization enthalpy and entropy, which also includes the electronic degeneracy factor, as $E_{DX} = H_{DX} - TS_{DX}$. The occupation of the shallow and deep donor levels, which determine the number of free carriers $n = n_d^+ - n_{DX}^- - N_A$, is given by the condition that they are in equilibrium with the states of the conduction band (N_A denotes the acceptor concentration).³⁷

To obtain the number of free carriers, the electron distribution was integrated numerically, and the occupation of the indirect valleys of the conduction band was included. The band structure, which is based on the available experimental data and interpolation between the values determined for GaAs and AlAs, was adopted from Ref. 38, where it is discussed in detail. We should note that the band-structure parameters for the higher-lying conduction-band valleys, the occupation of which becomes important in this temperature range, are somewhat uncertain. However, the purpose is to show that the disappearance of the vacancy signal is consistent with the ionization of the Si- DX center rather than to determine the thermal ionization energies.

The core-annihilation parameter is calculated from Eqs. (1)–(3), in which the concentration of positron traps C_D is now given by the occupation of the DX level (n_{DX}^-). The temperature dependence of the free-positron-annihilation parameter W_B was included. The core-annihilation parameter W_D for the defect state is independent of temperature. In the analysis the ionization enthalpy H_{DX} and the entropy S_{DX} , which are assumed to

be independent of temperature, and the positron trapping coefficient μ were considered as adjustable parameters. For the shallow level the enthalpy and entropy values $H_h = 9$ meV and $S_h = -0.06$ meV/K from far-infrared absorption and Hall data for $\text{Al}_x\text{Ga}_{1-x}\text{As}$ with a very similar alloy composition were used.³⁷ The acceptor concentration was taken as $N_A = 0$.

Figure 7 shows the core-annihilation parameters from 300 to 600 K in the Si-doped layer $x = 0.29$. The solid line indicates the core-annihilation parameter calculated assuming that the DX level occupies two electrons. The core-annihilation parameter was finally calculated by fixing the ionization enthalpy to $H_{DX} = 70$ meV. It is based on Hall experiments below 300 K which yield the value 73 meV for the Si- DX center at the same alloy composition.³⁷ The values obtained for the entropy and the trapping coefficient are $S_{DX} = 0.14$ meV/K and $\mu = 2 \times 10^{15}$ s⁻¹. The calculated electron concentration $n(300 \text{ K}) = 5 \times 10^{17}$ cm⁻³ is in good agreement with the experimental Hall carrier concentration 6.1×10^{17} cm⁻³.

This analysis of the annihilation parameters provides a useful insight into the identification of the vacancy defect. The ionization energies and the positron trapping coefficients are very consistent with other experiments. To obtain a satisfactory fit to the data with ionization

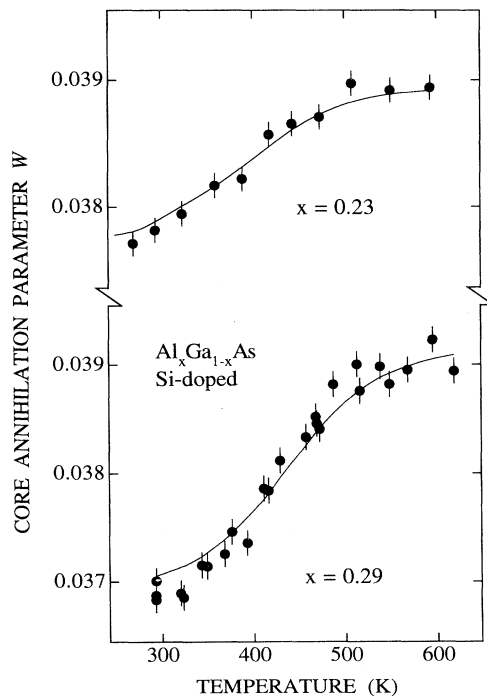


FIG. 7. The core-annihilation parameter W vs temperature at 300–600 K in the Si-doped $\text{Al}_x\text{Ga}_{1-x}\text{As}$ layers (a) $x = 0.29$ and (b) $x = 0.23$. The solid lines are calculated assuming that the donor impurity gives rise to a hydrogenic level and a deep level, and that positrons are trapped at the DX center when the deep electron level is occupied. In the calculation two electron occupation of the DX center was assumed. The thermal binding energies and the positron trapping rates are given in the text.

enthalpies taken from Hall experiments requires rather large and positive entropy values. As the entropy also includes the electronic degeneracy factor which makes a negative contribution to S_{DX} , it would indicate a large vibrational entropy term in the thermal activation energy. The Hall measurements below 300 K also yield a large positive entropy term 0.06 meV/K.³⁷ The trapping coefficient 2×10^{15} s⁻¹ is in perfect agreement with the typical values found earlier for positron capture at vacancies in semiconductors.^{25–28}

The same analysis was carried out assuming that only one electron is captured at the deep electron level. If the ionization enthalpy is fixed to $H_{DX} = 105$ meV, such a model yields $S_{DX} = 0.16$ meV/K and $\mu = 1 \times 10^{15}$ s⁻¹. Analysis of the Hall data³⁷ gives $H_{DX} = 109$ meV, and $S_{DX} = 0.14$ meV/K. Agreement with the experimental data is as good as for the model which assumes a two-electron occupation of the DX level in Fig. 7. Therefore, independent of the charge state of the DX center, the disappearance of the vacancy signal is consistent with the Hall experiments, and in both cases the trapping coefficients are consistent with the values in the literature.

A similar analysis was done for the Si-doped layer with a lower AlAs fraction $x = 0.23$ (Fig. 7). Here the same defect parameter W_D/W_B as in the layer $x = 0.29$ was assumed. The solid line in Fig. 7 corresponds to thermal ionization enthalpy $H_{DX} = 20$ meV, entropy $S_{DX} = 0.08$ meV/K, and the trapping coefficient $\mu = 1.8 \times 10^{15}$ s⁻¹. The DX center was assumed to bind two electrons, but the two models (one- and two-electron occupation of the DX level) yield equally good agreement with the experiment. The thermal ionization energy is clearly smaller than in the layer $x = 0.29$. The entropy term is positive and rather large, and the thermal ionization energy would indicate that the DX level is very close to the Γ edge of the conduction band at 300 K. This is consistent with the change of the DX center from a resonant level in the conduction band to a localized level in the band gap at the alloy composition $x \approx 0.22$.

In conclusion, we find that the thermal ionization of the Si- DX center explains the vanishing of the vacancy signal at $T > 300$ K. The thermal ionization energies estimated from the positron experiments are consistent with earlier Hall experiments below 300 K.

D. The DX center in $\text{Al}_x\text{Ga}_{1-x}\text{As}$ with $x < 0.25$

Positron trapping at vacancies was observed in Si-doped $\text{Al}_x\text{Ga}_{1-x}\text{As}$ with $x = 0.18$ (Fig. 1).¹⁴ Persistent photoquenching of positron trapping is seen below 100 K, leaving no doubt that the vacancy is the same as that found at the higher Al concentrations. This observation is related to the high Si concentration. The DX center is expected to be formed when at high doping concentration the Fermi level reaches the DX level in the conduction band. Occupation of this level is seen even in very heavily doped GaAs.³⁹ In DLTS experiments thermally activated capture is observed, and there is a large persistent photoconductivity effect characteristic of the DX center.⁴⁰ For $x = 0.18$ this condition is met when the

concentration is $2 \times 10^{18} \text{ cm}^{-3}$. It appears from the persistent photoconductivity effect⁴⁰ that the concentration of the *DX* center is approximately 50% of the total donor concentration at $x = 0.195$, and that persistent photoconductivity is observed even at $x = 0.15$.

The influence of the Al concentration on the number of vacancies can be seen by comparing the Si-doped layers $x = 0.18$ and 0.23 in which the Si concentrations are equivalent. At the alloy composition $x = 0.23$, the *DX* level is very close to the bottom of the conduction band. The metastable vacancy is observed, but the core-annihilation parameter W/W_B is larger than in the layers $x = 0.29$ or 0.61 . As in the layer $x = 0.18$, this indicates a smaller vacancy concentration. It appears that when the AlAs fraction is $x < 0.25$, the number of vacancies in the layers with the same donor concentration is correlated to the Al concentration. This can be understood by the fact that the *DX* level is pushed closer to and finally into the conduction band, and thereby the occupation of this level decreases.

E. Conclusions

We now make a summary of the properties of the vacancy in Si-doped $\text{Al}_x\text{Ga}_{1-x}\text{As}$ as they appear from the experimental results and the analysis presented above. The vacancy is connected with *n*-type doping and Al alloying. It cannot be observed in *n*-type GaAs or undoped $\text{Al}_x\text{Ga}_{1-x}\text{As}$. The vacancy concentration decreases in the *n*-type layers in which the Si concentration is $[\text{Si}] \approx 2.5 \times 10^{18} \text{ cm}^{-3}$ when the Al fraction is lowered to $x \approx 0.20$. At this range of the alloy composition the *DX* level becomes a resonant level. Positron trapping at the vacancy can be persistently removed by illumination with IR light. The optical cross section for this process is equal to the photoionization cross section for the Si-*DX* center in $\text{Al}_x\text{Ga}_{1-x}\text{As}$. The critical temperature below which the vacancy signal can be persistently removed and the temperature below which persistent photoconductivity is observed are identical. The electron-capture barrier at the *DX* center can explain the variation of the critical temperature with donor species (Si, Sn) (Ref. 14) and alloy composition ($0.2 \leq x \leq 0.6$). The disappearance of the vacancy at high temperatures coincides with the thermal ionization of the *DX* center, as indicated by the thermal ionization energies inferred from the Hall measurements below room temperature.

The analysis of the experiments gives a convincing indication of a marked correlation between the vacancy and the *DX* center. Positron trapping at the *DX* center provides a consistent way to explain *all* the experimental results. As indicated above, it is compatible also with the charge states of the *DX* center.

VI. MICROSCOPIC STRUCTURE OF THE Si-*DX* CENTER

In this section we will examine the microscopic structure of the Si-*DX* center, discuss the temperature dependence of positron trapping which indicates the negative

charge of the vacancy, and finally compare the structural data with the vacancy-interstitial model.

A. Structure

For the Si-*DX* center, we take the valence- and core-annihilation parameters S_D and W_D of the defect state as the values measured at 20 K in the layers $x = 0.29$ and 0.61 . In assigning the above values to positron annihilation at the *DX* center we assume that the positron trapping is saturated. In the Si-doped layer $x = 0.29$ the concentration of the *DX* centers is $C_{DX} \sim 10^{18} \text{ cm}^{-3}$. With the positron trapping coefficient $\mu \approx 2 \times 10^{15} \text{ s}^{-1}$ at room temperature, it yields the trapping rate $\kappa \sim 5 \times 10^{10} \text{ s}^{-1}$ which is an order of magnitude higher than the free-positron-annihilation rate λ_B . The fraction of positrons annihilating at the *DX* center is therefore $\kappa/(\kappa + \lambda_B) \sim 1$. The constant annihilation parameters below 300 K are also consistent with the saturation trapping. Measurement at 20 K after illumination directly gives the core-annihilation parameter for free positron annihilation. This yields $S_D/S_B = 1.0039(5)$ and $W_D/W_B = 0.937(3)$ when $x = 0.29$, and $1.0041(5)$ and $0.935(3)$ when $x = 0.61$. These values appear to be independent of the alloy composition, although W_B and W_D both vary with the AlAs mole fraction.

The positron lifetime gives a measure of the size of the vacancy, which is determined by the geometry of the defect and the relaxations of the neighboring ions. Annihilation with the core electrons is also influenced by the type of ions around the vacancy. This effect may be substantial in compound semiconductors if the core electron structures of the constituent atoms are very different, and it can be used to identify the vacancy.⁴¹ In GaAs, however, vacancies in either sublattice yield very similar Doppler parameters and, as indicated by the lifetimes, they are largely determined by the size of the vacancy. For the Ga vacancy V_{Ga} in electron-irradiated GaAs the core- and valence-annihilation parameters $W_D/W_B = 0.87$ and $S_D/S_B = 1.015 - 1.019$ have previously been determined.^{15,16} The positron lifetime at V_{Ga} is 260 ps.²³ In the negative-As vacancy V_{As} , which has a very similar lifetime of 257 ps,¹⁸ the core- and valence-annihilation parameters are $W_D/W_B = 0.89(1)$ and $S_D/S_B = 1.015(1)$.²³ In the neutral As vacancy the positron lifetime 295 ps (Ref. 18) indicates a large open volume, and it is also seen in the Doppler parameters $W_D/W_B = 0.80$ and $S_D/S_B = 1.030$.²³

In the case of the vacancy associated with the *DX* center the valence- and core-annihilation parameters are between those for free positron annihilation and those attributed to V_{Ga} or V_{As} in GaAs. The Doppler parameters therefore indicate that the vacancy associated with the Si-*DX* center is smaller than an isolated vacancy. This result can be understood if the vacancy is part of a complex, or if the nearest-neighbor ions are strongly relaxed. A similar conclusion was reached from the positron lifetime experiments in Te-doped $\text{Al}_x\text{Ga}_{1-x}\text{Sb}$ ⁴² which shows a smaller increase of the defect lifetime at the Te-*DX* center than, e.g., at vacancies in GaAs.

B. Negative charge state of the vacancy

Positron trapping into vacancies in different charge states was calculated by Puska, Corbel, and Nieminen.²⁸ They considered capture mechanisms involving both electron and phonon excitations. For a neutral vacancy the positron trapping coefficient μ is generally independent of temperature. For a negative vacancy the temperature dependence of the positron trapping coefficient is close to $T^{-1/2}$. This temperature dependence is a direct consequence of the Coulomb wave character of the initial positron state. The square of the amplitude of the initial positron wave function at the center of a negatively charged vacancy is inversely proportional to the thermal positron velocity leading to the temperature dependence $T^{-1/2}$ of the trapping coefficient. One can also draw an analogy between positron trapping at a negatively charged vacancy and the hole capture at negatively charged acceptors. Recently Darken and Jellison⁴³ reported hole capture cross sections for different singly and doubly ionized acceptors in high-purity Ge. They find that for several centers and different charge states the hole capture cross section depends only on temperature, and that it is proportional to T^{-1} corresponding to a capture rate proportional to $T^{-1/2}$.

The core-annihilation parameters between 20 and 150 K at different alloy compositions in the Si-doped $\text{Al}_x\text{Ga}_{1-x}\text{As}$ layers were indicated in Fig. 4. We will examine the temperature dependence of the positron trapping rate κ in the layers $x = 0.18$ and 0.23 , in which positron trapping is not saturated and the activation energies for electron capture and emission at the DX center are relatively large.

We calculate the positron trapping rates from the kinetic trapping model. The experimental data plotted in Fig. 4 suggests that the two-state model may not be sufficient to explain the temperature dependence. From 150 to 100 K the number of positrons annihilating at the DX center in the layers $x = 0.18$ and 0.23 actually decreases. It is very difficult to reconcile this with positron trapping at a vacancy. One possible cause is a competitive positron trapping at negatively charged ion-type centers in which the annihilation characteristics are nearly identical with free positron annihilation. Such centers are commonly observed in GaAs at low temperatures.^{18,23} If the trapping rate at the negative ions is κ_{st} , the kinetic trapping model yields the positron trapping rate

$$\kappa(T) = [\lambda_B + \kappa_{st}(T)] \frac{W(T) - W_B(T)}{W_D - W(T)}, \quad (7)$$

at the vacancies. When using Eq. (4) to calculate the trapping rate in order to estimate the optical cross sections (Sec. V A), negative ion-type centers were deliberately neglected. The true trapping rate at the vacancies may therefore be higher than what was indicated in Fig. 5, but the negative ions do not change the time decay of the trapping rate at vacancies as long as κ_{st} remains constant. The optical cross sections given in Sec. V A, therefore, remain unchanged.

We use Eq. (7) to calculate the trapping rates $\kappa(T)/[\lambda_B + \kappa_{st}(T)]$ at low temperatures $T < 100$ K. This

requires that the core-annihilation parameters $W_B(T)$ and W_D are known. The core-annihilation parameter $W_B(T)$ for free positron annihilation from 20 to 100 K was measured in each layer after illumination. It is shown in Fig. 4 for the layers $x = 0.18$ and 0.23 . The core-annihilation parameter for the defect state is taken from the layers $x = 0.29$ and 0.61 in which there is evidence of saturation trapping (Sec. VI A), i.e., we assume that $W_D/W_B = 0.936$ is independent of the AlAs fraction. As indicated in Fig. 4, the core-annihilation parameter W_D is independent of temperature.

Figure 8 shows $\kappa/(\lambda_B + \kappa_{st})$ as a function of temperature. If the trapping rate at negative ions is $\kappa_{st} > 0$, the true trapping rate at the DX center is higher. Also, as κ_{st} always increases when temperature is lowered,²⁸ the trapping rate at the DX center possibly increases even more rapidly at low temperatures than indicated in Fig. 8. Nevertheless, the decrease of the core-annihilation parameter at low temperatures can only follow from the increase of the positron trapping rate at the DX center. The electron-capture rate at the DX center is exceedingly small below 70 K, and there is no electron transfer between the deep level and the conduction band at low temperatures. We also note that in order to explain the increase of the positron trapping rate, the Si- DX concentration should increase by a factor of 2 between 80 and 20 K. However, the Hall carrier concentration in the layer $x = 0.23$ decreases only from 1.5 to $1.4 \times 10^{18} \text{ cm}^{-3}$ between 100 and 50 K, and it remains constant from 50 to 12 K, indicating that the number of electrons captured at the DX level is very small. We conclude that the number

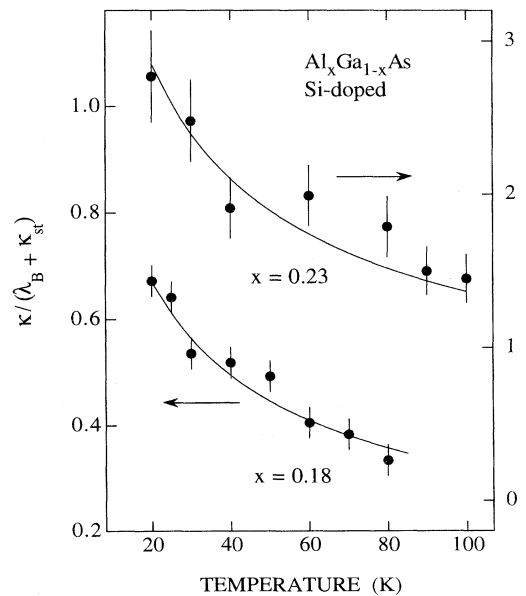


FIG. 8. Plot showing the position trapping rate vs temperature from 20 to 100 K in Si-doped $\text{Al}_x\text{Ga}_{1-x}\text{As}$ layers $x = 0.18$ and 0.23 . Here λ_B is the free positron-annihilation rate, and κ_{st} is the trapping rate at negative ion-type centers; see Eq. (7). The solid lines indicate the temperature dependence $T^{-1/2}$.

of vacancies remains constant below 80 K, and the increase of the positron trapping rate is attributed to the temperature dependence of the positron trapping coefficient.

We use the positron trapping rate $\kappa(T)$ to discriminate between neutral and negative charge states of the vacancy. Although the mechanism of energy dissipation is not clear, the divergence of the trapping coefficient at low temperatures implies positron trapping at a long-range attractive defect potential. This finding directly indicates the negative charge of the vacancy.

The question of the total charge of the *DX* center is more subtle. As positron annihilation at low temperatures includes some contribution from negative ion-type centers, we cannot attribute the temperature dependence $T^{-1/2}$ (Fig. 8) characteristic of positron trapping at the Coulomb potential to the *DX* center. In that case the temperature dependence of the trapping rate does not definitely rule out the neutral charge state of the *DX* center. Positron trapping at the EL2 defect provides a counterexample. In semi-insulating GaAs the trapping rate at the metastable configuration of the EL2 defect which is electrically neutral depends strongly on temperature.^{15,16} It was suggested that a negatively charged vacancy which is a part of a neutral defect complex may also lead to temperature-dependent trapping rate.

C. Comparison with theoretical models

Positron experiments indicate the vacancylike structure of the Si-*DX* center. In conjunction with some earlier experiments, this finding provides useful insight into the metastability of the donor impurity. It is generally accepted that once the *DX* center is ionized at low temperatures, the Si atom is at a substitutional Ga site. The shallow hydrogenic states of the substitutional Si atom have been seen in infrared absorption,^{44,45} Hall,^{37,46} and electron paramagnetic resonance⁴⁷⁻⁴⁹ measurements. Moreover, it has been shown that the *DX* levels and the hydrogenic levels originate from the same impurity atom.⁴⁴ Therefore large atomic displacements are necessary to explain the vacancy-type nature of the *DX* center when the deep donor level is occupied. This gives direct proof of the large lattice relaxation upon electron capture which has been invoked to explain the metastability.

It has become increasingly evident that the vacancy-interstitial model⁵⁻⁹ accounts for the electrical and optical properties of the *DX* center. The calculated atomic structure is characterized by a large displacement of the column-IV donor atom along the $\langle 111 \rangle$ direction into a threefold-coordinated position. In the case of Si, the center involves a 1.17-Å displacement of the Si atom, and the distorted geometry can be viewed as a pair of a Ga vacancy and a Si interstitial in which the Si atom is off center.

The vacancy-interstitial model is consistent with the structural data from positron-annihilation experiments. It predicts the formation of a vacant Ga site. Obviously, this is in agreement with the positron experiments which directly indicate the vacancylike structure of the *DX* center. The impurity atom at an interstitial site next to

the vacancy would also account for the fact that the open volume is not as large as in case of an isolated Ga vacancy. Positron lifetimes at the *DX* center in GaAs have been calculated assuming the ionic structure predicted by the vacancy-interstitial model.⁵⁰ It indicates that the vacant Ga site in a close V_{Ga} -Si pair can bind a positron into a localized state. If the positron lifetime at the Ga vacancy is adjusted to 264 ps, in agreement with its experimental value 260 ps,²³ by setting the positron effective mass to $m^* = 1.5m_e$, the lifetime at the Si-*DX* center is 253 ps. The difference in the core-annihilation parameters for V_{Ga} and the Si-*DX* center corresponds very well to the theoretical defect lifetimes.

The variation of the core-annihilation parameter W_D with the alloy composition is very similar to free positron annihilation. It suggests that the Ga atoms also make a large x -dependent contribution to the core electron annihilation at the *DX* center. This observation is not in contradiction to the vacancy-interstitial model, even if the nearest neighbors around the vacancy are As atoms. It can be traced back to the rather weak localization of the positron at the *DX* center, as indicated by the calculated positron wave function.⁵⁰ One therefore expects a large contribution to the core electron annihilation from Ga and Al atoms in the Ga sublattice.

The charge state of the *DX* center bears a close relation to its microscopic structure. Khachatryan, Weber, and Kaminska⁵¹ proposed a two-electron negative- U state of the donor to explain the persistent photoconductivity and the absence of the EPR signal of the *DX* centers. The same conclusion was reached by Chadi and Chang⁷ from self-consistent pseudopotential total-energy calculations. They found the *DX* center is a highly localized and negatively charged center. A negative total charge would give a straightforward explanation to the increase of the positron trapping rate at the Si-*DX* center at low temperatures. However, as discussed in Sec. V, section, by the present experimental data one cannot judge the temperature dependence of the positron trapping rate to be a proof of the negative charge state.

We finally point out the similarity of the *DX* center with the EL2 center in GaAs. It has been verified that an As antisite is a part of the stable state of the EL2 center.⁵² The metastability of the EL2 center has been associated with the large displacement of the As atom into the neighboring interstitial site.^{5,6} Therefore the atomic structure of the metastable state of the EL2 center is very similar to the structure of the Si-*DX*. Positron experiments^{15,16} have shown that the metastable configuration of the EL2 center contains a vacancy. The annihilation parameters are quite similar in the two cases, suggesting that the atomic configurations of the *DX* center and the metastable state of EL2 are very similar. The displacement of the column-IV donor atom (*DX*) or the As atom (EL2) from the Ga site predicted by the vacancy-interstitial model therefore gives a consistent picture of positron annihilation at these metastable defects.

VII. SUMMARY

We have applied positron-annihilation spectroscopy to investigate the microscopic structure and the charge state

of the *DX* center in Si-doped $\text{Al}_x\text{Ga}_{1-x}\text{As}$ grown by molecular-beam epitaxy. In agreement with our earlier experiments all Si-doped $\text{Al}_x\text{Ga}_{1-x}\text{As}$ layers were found to contain vacancy-type defects. The vacancy was observed only in *n*-type layers with the AlAs mole fraction $x \geq 0.18$.

After illumination with IR light (photon energy ~ 1.3 eV) the vacancy signal disappears persistently. The optical cross section for this process is equal to the photoionization cross section for the Si-*DX* center. The temperature at which the vacancy recovers depends on the AlAs mole fraction. It was found to be in good agreement with the variation of the electron-capture barrier at the *DX* center. The disappearance of the vacancy signal in thermal equilibrium above room temperature coincides with thermal ionization of the *DX* center. The electron binding energies estimated from the positron-annihilation data are consistent with those found from the Hall experiments below room temperature. We conclude that the vacancy defect observed in Si-doped $\text{Al}_x\text{Ga}_{1-x}\text{As}$ is the Si-*DX* center.

By showing the vacancylike structure of the Si-*DX* center, positron annihilation provides additional information about the local structure of the *DX* center. The vacancy is smaller in size than an isolated vacancy in GaAs. These results also provide insight into the metastability of the *DX* center. Earlier experiments have indicated that once the *DX* is ionized, the Si impurity is at the substitu-

tional Ga site. The vacancy-type nature of the *DX* center shows directly that ionic configurations corresponding to the different electronic configurations must be totally different. The structural data from positron experiments are in good agreement with theoretical calculations which predict a large displacement of the group-IV impurity into a threefold-coordinated interstitial site. The temperature dependence of the positron trapping rate shows that the vacancy is negatively charged. This is consistent with the two-electron occupation if the deep donor level predicted by the vacancy-interstitial model.

Theoretical studies have suggested that different forms of *sp* hybridization in covalent crystals are responsible for the metastability of the donor impurities. The same basic mechanism has been used to explain the metastability of the EL2 center in GaAs. We note that the displacement of the column-IV donor atom (*DX*) or the As atom (EL2) from the Ga site predicted by the vacancy-interstitial model gives a consistent picture of positron annihilation at these metastable defects.

ACKNOWLEDGMENTS

We thank Y. Druelle and J. L. Lorriaux (Université des Sciences et Techniques de Lille) and M. Toivonen (Tampere University of Technology) for some of the MBE-grown layers, and M. Puska and R. M. Nieminen for fruitful discussions and comments.

-
- ¹D. V. Lang and R. A. Logan, *Phys. Rev. Lett.* **39**, 635 (1977).
²D. V. Lang, R. A. Logan, and M. J. Jaros, *Phys. Rev. B* **19**, 1015 (1979).
³P. M. Mooney, *J. Appl. Phys.* **67**, R1 (1990).
⁴*Physics of DX Centers in GaAs Alloys*, edited by J. C. Bourgoin (Sci-Tech, Lake Isabella, CA, 1990).
⁵J. Dabrowski and M. Scheffler, *Phys. Rev. Lett.* **60**, 2183 (1988).
⁶D. J. Chadi and K. J. Chang, *Phys. Rev. Lett.* **60**, 2187 (1988).
⁷D. J. Chadi and K. J. Chang, *Phys. Rev. Lett.* **61**, 873 (1988).
⁸M. J. Caldas, J. Dabrowski, A. Fazzio, and M. Scheffler, *Phys. Rev. Lett.* **65**, 2046 (1990).
⁹J. Dabrowski and M. Scheffler, in *Defects in Semiconductors*, edited by G. Davies, G. L. DeLeo, and M. Stavola, *Material Science Forum Vols. 83-87* (Trans Tech, Brookfield, 1992), p. 735.
¹⁰M. Saito, A. Oshiyama, and O. Sugino, *Phys. Rev. B* **45**, 13 745 (1992).
¹¹D. J. Chadi, *Phys. Rev. Lett.* **72**, 534 (1994).
¹²*Positrons in Solids*, edited by P. Hautojärvi, *Topics in Current Physics Vol. 12* (Springer-Verlag, Heidelberg, 1979).
¹³*Positron Solid State Physics*, edited by W. Brandt and A. Dupasquier (North-Holland, Amsterdam, 1983).
¹⁴J. Mäkinen, T. Laine, K. Saarinen, C. Corbel, V. M. Airaksinen, and P. Gibart, *Phys. Rev. Lett.* **71**, 3154 (1993).
¹⁵R. Krause, K. Saarinen, P. Hautojärvi, A. Polity, G. Gärtner, and C. Corbel, *Phys. Rev. Lett.* **65**, 3329 (1990).
¹⁶K. Saarinen, S. Kuisma, P. Hautojärvi, C. Corbel, and C. LeBerre, *Phys. Rev. B* **49**, 8005 (1994).
¹⁷P. J. Schultz and K. G. Lynn, *Rev. Mod. Phys.* **60**, 701 (1988).
¹⁸K. Saarinen, P. Hautojärvi, P. Lanki, and C. Corbel, *Phys. Rev. B* **44**, 10 585 (1991).
¹⁹C. Corbel, M. Stucky, P. Hautojärvi, K. Saarinen, and P. Moser, *Phys. Rev. B* **38**, 8192 (1988).
²⁰M. J. Puska (private communication).
²¹M. J. Stott and R. N. West, *J. Phys. F* **8**, 635 (1978).
²²C. Corbel, F. Pierre, K. Saarinen, P. Hautojärvi, and P. Moser, *Phys. Rev. B* **45**, 3386 (1992).
²³R. Ambigapathy, A. A. Manuel, P. Hautojärvi, K. Saarinen, and C. Corbel, *Phys. Rev. B* **50**, 2188 (1994).
²⁴R. N. West, in *Positrons in Solids* (Ref. 13), p. 89.
²⁵J. Mäkinen, C. Corbel, P. Hautojärvi, P. Moser, and F. Pierre, *Phys. Rev. B* **39**, 10 162 (1989).
²⁶J. Mäkinen, P. Hautojärvi, and C. Corbel, *J. Phys. Condens. Matter* **3**, 7217 (1991).
²⁷R. Krause, A. Klimakow, F. M. Kiesling, A. Polity, P. Gille, and M. Schenk, *J. Cryst. Growth* **101**, 512 (1990).
²⁸M. J. Puska, C. Corbel, and R. M. Nieminen, *Phys. Rev. B* **41**, 9980 (1990).
²⁹P. M. Mooney, G. A. Northrop, T. N. Morgan, and H. G. Grimmeiss, *Phys. Rev. B* **37**, 8298 (1988).
³⁰G. A. Northrop and P. M. Mooney, *J. Electron. Mater.* **20**, 13 (1991).
³¹R. Legros, P. M. Mooney, and S. L. Wright, *Phys. Rev. B* **35**, 7505 (1987).
³²H. G. Grimmeiss, *Annu. Rev. Mater. Sci.* **7**, 341 (1977).

- ³³P. M. Mooney, N. S. Caswell, and S. L. Wright, *J. Appl. Phys.* **62**, 4786 (1987).
- ³⁴P. M. Mooney, T. N. Theis, and S. L. Wright, *Appl. Phys. Lett.* **53**, 2546 (1989).
- ³⁵P. M. Mooney, T. N. Theis, and E. Calleja, *J. Electron. Mater.* **20**, 23 (1991).
- ³⁶E. Munoz and E. Calleja, in *Physics of DX Centers in GaAs Alloys* (Ref. 4), p. 99.
- ³⁷T. N. Theis, P. M. Mooney, and B. D. Parker, *J. Electron. Mater.* **20**, 35 (1991).
- ³⁸M. Guzzi and J. L. Staehli, in *Physics of DX Centers in GaAs Alloys* (Ref. 4), p. 25.
- ³⁹T. N. Theis, P. M. Mooney, and S. L. Wright, *Phys. Rev. Lett.* **60**, 361 (1988).
- ⁴⁰T. Ishikawa, T. Yamamoto, and K. Kondo, *Jpn. J. Appl. Phys.* **25**, L484 (1986).
- ⁴¹M. Alatalo, H. Kauppinen, K. Saarinen, M. J. Puska, J. Mäkinen, P. Hautojärvi, and R. M. Nieminen, *Phys. Rev. B* **51**, 4176 (1995).
- ⁴²R. Krause-Rehberg, Th. Drost, A. Polity, G. Roos, G. Pensl, D. Volm, B. K. Meyer, G. Bischofink, and K. W. Benz, *Phys. Rev. B* **48**, 11 723 (1993).
- ⁴³L. S. Darken and G. E. Jellison, Jr., *Appl. Phys. Lett.* **55**, 1424 (1989); L. S. Darken, *Phys. Rev. Lett.* **69**, 2839 (1992).
- ⁴⁴T. N. Theis, T. F. Kuech, L. Palmateer, and P. M. Mooney, in *Gallium Arsenide and Related Compounds*, edited by B. de Cremoux, IOP Conf. Proc. No. 74 (Institute of Physics and Physical Society, Bristol, 1984).
- ⁴⁵J. E. Dmochowski, J. E. Dobaczewski, L. Dobaczewski, J. M. Langer, and W. Jantsch, *Phys. Rev. B* **40**, 9671 (1989).
- ⁴⁶M. Mizuta and K. Mori, *Phys. Rev. B* **37**, 1043 (1988).
- ⁴⁷P. M. Mooney, W. Wilkening, U. Kaufmann, and T. F. Kuech, *Phys. Rev. B* **39**, 5554 (1989).
- ⁴⁸H. J. von Bardeleben, J. C. Bourgoin, P. Basmajji, and P. Gibart, *Phys. Rev. B* **40**, 5892 (1989).
- ⁴⁹K. Khachatryan, E. R. Weber, M. G. Crawford, and G. E. Stillman, *J. Electron. Mater.* **20**, 59 (1991).
- ⁵⁰M. Puska (private communication); a similar calculation for the EL2 center in GaAs has been published in K. Laasonen, M. Alatalo, M. J. Puska, and R. M. Nieminen, *J. Phys. Condens. Matter* **3**, 7217 (1991).
- ⁵¹K. Khachatryan, E. R. Weber, and M. Kaminska, *Proceedings of the 15th International Conference on Defects in Semiconductors* [*Mater. Sci. Forum* **38-41**, 1067 (1989)].
- ⁵²G. M. Martin and S. Makram-Ebeid, in *Deep Centers in Semiconductors*, edited by S. T. Pantelides (Gordon and Breach, New York, 1986), p. 399.